Enhancement of the phase-measurement sensitivity beyond the standard quantum limit by a nonlinear interferometer

Z. Y. Ou*
Department of Physics, Indiana University-Purdue University Indianapolis, 402 N. Blackford Street, Indianapolis, Indiana 46202, USA
(Received 31 March 2011; published 14 February 2012)

A nonlinear interferometer uses nonlinear elements as beam splitters to split and to recombine optical waves for interference. As a result, the interference fringe size has a nonlinear dependence on the intensity of the field for phase sensing and leads to an enhanced phase signal. In this paper, a practical scheme of nonlinear interferometry for precision phase measurement is analyzed with parametric amplifiers as the nonlinear beam splitters. It is found that the signal due to phase shift is enhanced by a factor of the amplification gain as compared to a linear interferometer with the same phase-sensing light intensity while the quantum noise is kept at the vacuum level, thus, effectively increasing the signal-to-noise ratio (SNR) beyond the standard quantum limit. Furthermore, the scheme is not as sensitive to the detection loss as the linear scheme with a squeezed state for noise reduction. However, losses inside the interferometer limit the enhancement factor in SNR. We apply the concept to a Michelson interferometer but with parametric amplifiers involved for gravitational-wave detection. We find that effective power is increased by the gain of the amplifiers without actually increasing the cycling power inside the interferometer. Furthermore, the full benefits with squeezed input and variational output or the combination of a quantum nondemolition interferometer for sensitivity beyond the standard quantum limit apply here with even better results. Such a nonlinear interferometer will find wide applications in precision measurements.

DOI: 10.1103/PhysRevA.85.023815 PACS number(s): 42.50.St, 07.60.Ly, 42.50.Lc, 42.65.Yj

I. INTRODUCTION

More than a century ago, Michelson and Morley [1] performed a precision phase measurement with the invention of their interferometer. The result played a critical role in the development of Einstein's special relativity. Since then, optical interferometry has been refined with its sensitivity ever increasing and now reaching the quantum limit. But the fundamental design of an optical interferometer never has been changed. Even with the advent of quantum sources, such as squeezed states [2], the basic elements are still beam splitters for splitting and recombining waves. The only difference is the reduction in quantum noise via squeezed states [3–7]. The state of the art is the Laser Interferometer Gravitational-Wave Observatory (LIGO) project [8,9] whose application is to test yet another theory of Einstein, i.e., the general relativity.

Another line of research follows the trail of a special kind of state called the NOON state, which is a maximally entangled state of photon numbers [10]. The phase-measurement sensitivity is increased because the phase signal is enhanced by N times with N as the photon number. However, practical implementation is limited to a low number of photons because of the difficulty in generating the NOON state with a large photon number.

In the squeezed state approach mentioned above, attention is payed to the quantum states that are used in the interferometer but with the hardware structure of the interferometer unchanged. This is straightforward thinking after Caves pointed out, in a seminal paper [2], that quantum noise is the limiting factor in a traditional interferometer. So, most research effort is on finding the correct quantum states with various quantum correlations in order to increase the phase-measurement sensitivity or the signal-to-noise ratio (SNR) by reducing the noise.

On the other hand, there is another side to the story concerning sensitivity, that is, the signal side. The increase in the signal relies on the hardware or structure change in an interferometer. As a matter of fact, precision phase measurement is not confined to a traditional interferometer composed of beam splitters. A proposal by Yurke *et al.* [11] uses an SU(1,1) transformation (realized in parametric down-conversion processes) to split and to recombine the fields that carry phase information. Jacobson *et al.* [12] suggested using a cavity QED device to split a coherent state into a Schrödinger cat state and to form a nontraditional interferometer. Following these, a general protocol [13] was suggested using an arbitrary unitary transformation for phase measurement, that is, as shown in Fig. 1,

$$|\Psi\rangle_{\text{out}}(\varphi) = \hat{\mathcal{U}}^{\dagger} e^{i\varphi\hat{a}^{\dagger}\hat{a}}\hat{\mathcal{U}}|\Psi\rangle_{\text{in}}. \tag{1}$$

Here, $\hat{\mathcal{U}}$ can be any unitary operator that involves the phase-sensing mode $\hat{a}$, and $|\Psi\rangle_{\text{in}}$ is the initial input state. Thus, precision measurement of phase shift φ relies on differentiating states $|\Psi\rangle_{\text{in}}$ and $|\Psi\rangle_{\text{out}}(\varphi)$.

So, following our previous discussion on the SNR, input state $|\Psi\rangle_{\text{in}}$ is mostly responsible for quantum-noise reduction, whereas, the unitary operator, as we see later in the paper, is designed to increase the phase signal so as to enhance the SNR. Although there is a vast amount of research on input state $|\Psi\rangle_{\text{in}}$ for noise reduction, there are only a few on the unitary operator. As we see later, an appropriate unitary usually gives rise to a nonlinear dependence of interference fringe size on the phase-sensing field. It is the property that leads to the enhancement in the phase signal. So, we assign the name "nonlinear" to this type of interferometer. Note that it should not be confused with the name "nonlinear phase shift,"

*zou@iupui.edu

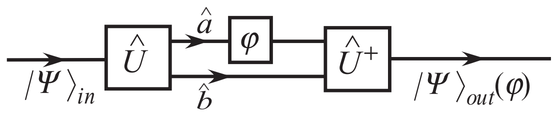

FIG. 1. General phase-measuring scheme with an arbitrary unitary operation as the generalized beam splitter.

which is introduced by a nonlinear interaction, such as the Kerr effect [14–16].

For a traditional interferometer, which is the benchmark to be compared to, beam splitters are used with $\hat{\mathcal{U}}$ being an SU(2) transformation [17]. Besides the SU(1,1) and SU(2) transformations, other unitary operators were proposed [12,13] and even were realized experimentally [18]. Some of the schemes can reach the ultimate quantum limit for phase measurement, i.e., the Heisenberg limit [19]. But most studies were at the theoretical level, and the sole experimental investigation [18] was at the low-photon level. Recently, a variation in the SU(1,1) interferometer with a coherent-state input was studied [20], and the nonlinear property of such an interferometer was demonstrated experimentally with signal-enhancement ability [21]. Thus, it holds great promise for an experimental implementation of the idea of using nonlinear processes for interferometry with greater sensitivity.

In this paper, we consider an experimentally implementable nonlinear interferometer studied in Refs. [20,21] that employs two parametric amplifiers to split and to recombine a strong coherent field. However, different from the analysis in Ref. [20], which uses photon-number detection, our detection scheme is the homodyne detection, which is the experimentally preferred method for quantum-noise measurement. Compared to Ref. [21], which only involves classical analysis, we analyze the quantum-noise performance of the nonlinear interferometer and find that, just as the argument in previous paragraphs suggests, the signal due to phase change is greatly enhanced because of the nonlinear nature of the interferometer. The enhancement factor is the power gain of the parametric amplifier. With its quantum-noise level at vacuum, the signal enhancement effectively increases the SNR above the standard quantum limit by the same factor. To imitate the environment of an actual experiment, we also study the effect of the losses on the enhancement factor and find that it is limited mainly by the losses inside the interferometer. Because the interferometer operates at vacuum-noise level, it is less sensitive to the loss at detection than the traditional interferometric scheme with squeezed-state input.

The paper is organized as follows. We first compare the noise performance of the linear and the nonlinear interferometers in Sec. II. Then, we analyze the effect of losses, both external and internal, in Sec. III. In Sec. IV, we apply the concept of the nonlinear interferometer to a modified Michelson interferometer for the application of gravitational-wave detection. We conclude in Sec. V with a summary and a discussion.

II. A NONLINEAR INTERFEROMETER WITH PARAMETRIC AMPLIFIERS

Consider the conceptual sketch in Fig. 2 where the one on the left [Fig. 1(a)] is a traditional linear interferometer, whereas, the one on the right is a nonlinear interferometer with parametric amplifiers as beam splitters. Assume that there is a coherent-state input at both interferometers. For the linear interferometer in Fig. 1(a), with the input-output relation for a lossless beam splitter given by

$$\begin{aligned}\hat{A} &= (\hat{a}_{\rm in} + \hat{b}_{\rm in})/\sqrt{2}, \quad \hat{B} = (\hat{b}_{\rm in} - \hat{a}_{\rm in})/\sqrt{2},\\ \hat{a}_{\rm out} &= (\hat{A} + \hat{B}e^{i\varphi})/\sqrt{2}, \quad \hat{b}_{\rm out} = (\hat{B}e^{i\varphi} - \hat{A})/\sqrt{2},\end{aligned} \tag{2}$$

it is straightforward to express the outputs of the interferometer in terms of the inputs,

$$\hat{a}_{\rm out} = t(\varphi)\hat{a}_{\rm in} + r(\varphi)\hat{b}_{\rm in}, \quad \hat{b}_{\rm out} = t(\varphi)\hat{b}_{\rm in} + r(\varphi)\hat{a}_{\rm in}, \tag{3}$$

where $t(\varphi) = e^{i\varphi/2}\cos\varphi/2$ and $r(\varphi) = ie^{i\varphi/2}\sin\varphi/2$. Here, φ is the phase change, and we assume the beam splitters are identical with 50:50 transmissivity and reflectivity.

For a coherent state $|\alpha\rangle$ input at $\hat{a}_{\rm in}$ and vacuum at $\hat{b}_{\rm in}$, the output of the interferometer is simply

$$\langle\hat{b}^{\dagger}_{\rm out}\hat{b}_{\rm out}\rangle = |\alpha|^2(1-\cos\varphi)/2 = I_{ps}(1-\cos\varphi), \tag{4}$$

where $I_{ps} \equiv \langle\hat{B}^{\dagger}\hat{B}\rangle = |\alpha|^2/2$ is the photon number of the field subject to the phase shift (phase-sensing field). Note that the phase-sensing field is what matters in phase-measurement accuracy as shown in Refs. [15,19]. The interferometer usually works at $\varphi = 0$ with a homodyne detection at the dark port, i.e., $\hat{b}_{\rm out}$. With a small phase shift δ for φ and $\alpha = i|\alpha|$, we easily can find

$$\begin{aligned}\left\langle\hat{X}^2_{b_{\rm out}}\right\rangle &= \left\langle\hat{X}^2_{b_{\rm in}}(\delta/2)\right\rangle\cos^2(\delta/2) + \left\langle\hat{Y}^2_{a_{\rm in}}(\delta/2)\right\rangle\sin^2(\delta/2)\\ &\approx 1 + |\alpha|^2\delta^2 \quad \text{for } \delta \ll 1,\ |\alpha|^2 \gg 1.\end{aligned} \tag{5}$$

Here, $\hat{X}_b(\delta/2) = \hat{b}e^{i\delta/2} + \hat{b}^{\dagger}e^{-i\delta/2}$ and $\hat{Y}_a(\delta/2) = (\hat{a}e^{i\delta/2} - \hat{a}^{\dagger}e^{-i\delta/2})/i$ are the quadrature-phase amplitudes of corresponding fields. Obviously, $|\alpha|^2\delta^2$ in $\langle\hat{X}^2_{b_{\rm out}}\rangle$ corresponds to the phase signal while the noise of the phase measurement is simply 1 from vacuum quantum noise. Hence, the SNR of the linear interferometer is

$$R_L = |\alpha|^2\delta^2/1 = 2I_{ps}\delta^2, \tag{6}$$

which leads to the standard quantum limit (SQL) $\delta_{\rm SQL} = 1/\sqrt{N}$ with $N = 2I_{ps}$.

For the nonlinear interferometer in Fig. 1(b), a parametric amplifier now acts as a beam splitter to split the input signal beam ($c_{\rm in}$) into the amplified signal beam (C) and the accompanying beam (D). Another parametric amplifier acts as a beam combiner to complete the interferometer. Even though there is no injection at mode $d_{\rm in}$ for the amplifier, vacuum still contributes with quantum noise (see Ref. [2]). The full input-output relation for the amplifiers is given by [22]

$$\begin{aligned}\hat{C} &= G\hat{c}_{\rm in} + g\hat{d}^{\dagger}_{\rm in}, \quad \hat{D} = G\hat{d}_{\rm in} + g\hat{c}^{\dagger}_{\rm in},\\ \hat{c}_{\rm out} &= G\hat{C} + g\hat{D}^{\dagger}e^{-i\varphi}, \quad \hat{d}_{\rm out} = G\hat{D}e^{i\varphi} + g\hat{C}^{\dagger},\end{aligned} \tag{7}$$

where we assume the amplifiers are identical with G as the amplitude gain and $|G|^2 - |g|^2 = 1$. Here, we introduce a phase shift in φ on mode $\hat{D}$. Therefore, the output-input relation of the interferometer is

$$\begin{aligned}\hat{c}_{\rm out} &= [G_T(\varphi)\hat{c}_{\rm in} + g_T(\varphi)\hat{d}^{\dagger}_{\rm in}]e^{-i\varphi},\\ \hat{d}_{\rm out} &= G_T(\varphi)\hat{d}_{\rm in} + g_T(\varphi)\hat{c}^{\dagger}_{\rm in},\end{aligned} \tag{8}$$

with $G_T(\varphi) = G^2 e^{i\varphi} + g^2$ and $g_T(\varphi) = Gg(1 + e^{i\varphi})$. The interferometer works best at a dark fringe with $\varphi = \pi$ when $G_T(\pi) = 1$ and $g_T(\pi) = 0$, i.e., at unit overall gain [11].

With a coherent-state input at $c_{\rm in}$ and no input at $d_{\rm in}$ as shown in Fig. 1(b), similar to Eq. (4), we easily can find the dark output port ($d_{\rm out}$) intensity as

$$\begin{aligned}\langle \hat{d}^\dagger_{\rm out}\hat{d}_{\rm out}\rangle &= |G_T(\varphi)|^2 + |g_T(\varphi)|^2(|\alpha|^2 + 1)\\ &\approx 2G^2 g^2 |\alpha|^2(1 + \cos\varphi) \quad \text{for} \quad |\alpha|^2 \gg 1\\ &= 2G^2 I^{nl}_{ps}(1 + \cos\varphi),\end{aligned} \tag{9}$$

where $I^{nl}_{ps} = \langle \hat{D}^\dagger \hat{D}\rangle = g^2(|\alpha|^2 + 1) \approx g^2|\alpha|^2(|\alpha|^2 \gg 1)$ is the photon number of the phase-sensing field $\hat{D}$. Comparing the above with Eq. (4) for a linear interferometer, we find that the fringe size is increased by a factor of $2G^2$.

For homodyne detection around the dark fringe with $\varphi = \pi + \delta$ ($\delta \ll 1$) and $\alpha = i|\alpha|$, we have, from Eqs. (7) and (8),

$$\begin{aligned}\langle \hat{X}^2_{d_{\rm out}}\rangle &= |G_T(\varphi)|^2\langle \hat{X}^2_{d_{\rm in}}(\varphi_G)\rangle + |g_T(\varphi)|^2\langle \hat{X}^2_{c_{\rm in}}(\varphi/2)\rangle\\ &\approx 1 + G^2 g^2(4|\alpha|^2 + 2)\delta^2 \quad \text{for} \quad \delta \ll 1,\end{aligned} \tag{10}$$

where $e^{i\varphi_G} \equiv G_T(\varphi)/|G_T(\varphi)|$. Hence, the SNR for the nonlinear interferometer then is

$$R_{NL} = G^2 g^2(4|\alpha|^2 + 2)\delta^2/1 \approx 4G^2 I^{nl}_{ps}\delta^2 \quad \text{for } |\alpha|^2 \gg 1. \tag{11}$$

Comparing this with Eq. (6), we find that, under the condition of the same number of photons for the phase-sensing field, the nonlinear interferometer has a better SNR than the linear interferometer with an enhancement factor of

$$R_{NL}/R_L \approx 2G^2 \quad \text{for} \quad |\alpha|^2 \gg 1. \tag{12}$$

The sensitivity of phase measurement for a linear interferometer is usually at the so-called SQL. Then, the nonlinear interferometer improves upon the SQL by $2G^2$-fold. The physical picture of this enhancement in sensitivity is straightforward if we compare the output fringe intensities in Eqs. (4) and (9) for the two interferometers: The fringe size is increased by a factor of $2G^2$. In the meantime, at $\varphi = 0$ (dark output), $\hat{d}_{\rm out} = \hat{d}_{\rm in}$, which is in vacuum, so the noise is simply vacuum noise just as in the linear interferometer. Thus, the improvement in sensitivity is achieved not by reducing the vacuum quantum noise at the unused input port, which usually is performed with a linear interferometer but rather by enhancing the signal level via amplification in the nonlinear interferometer.

With a squeezed vacuum at the unused input port ($\hat{d}_{\rm in}$), i.e., $\langle \hat{X}^2_{d_{\rm in}}\rangle = e^{-r}$, Eq. (10) is modified to

$$\langle \hat{X}^2_{d_{\rm out}}\rangle = e^{-r} + 4G^2 g^2|\alpha|^2\delta^2. \tag{13}$$

Then, the sensitivity of phase measurement can be increased further from the SQL by a factor of

$$R^S_{NL}/R_L = 2G^2 e^r. \tag{14}$$

Another interesting case is when there is no injection of the coherent state at all. Setting $|\alpha|^2 = 0$ in Eq. (11), we have the SNR without coherent injection,

$$R^{nc}_{NL} = 2G^2 g^2\delta^2 = 2I^{nl}_{ps}\left(I^{nl}_{ps} + 1\right)\delta^2. \tag{15}$$

This leads to the so-called Heisenberg limit [11,13],

$$\delta_m = 1\Big/\sqrt{2I^{nl}_{ps}\left(I^{nl}_{ps} + 1\right)} \approx 1/N, \tag{16}$$

with $N \equiv I^{nl}_{ps} \gg 1$ as the number of photons probing the phase shift. Squeezed-vacuum injection in the idler port can increase the SNR further, but the photon number also increases because squeezed vacuum contains photons.

III. LOSS ANALYSIS FOR THE NONLINEAR INTERFEROMETER

It is well known that loss is the limiting factor that hinders the application of the squeezed state in precision measurements. Next, let us examine the effect of loss on the sensitivity of this scheme of a nonlinear interferometer. There are two types of losses: inside and outside the interferometer. We start with loss outside the interferometer first.

A. Effect of loss outside the nonlinear interferometer

Loss outside the interferometer can be from propagation loss, less than perfect homodyne mode match, and most likely, the finite-quantum efficiency of the detectors. We can sum up all these losses to get an overall loss of L and model it by a beam splitter of transmissivity $(1 - L)$: $\hat{d}'_{\rm out} = \hat{d}_{\rm out}\sqrt{1 - L} + \hat{d}_0\sqrt{L}$. It is straightforward to find that Eq. (10) becomes

$$\langle \hat{X}^2_{d'_{\rm out}}\rangle = 1 + 4(1 - L)G^2 g^2|\alpha|^2\delta^2. \tag{17}$$

So the SNR is reduced by a factor of $1 - L$. Such a reduction can be compensated by the increase in gains (G,g). The sensitivity enhancement is unlimited.

Recall that, for squeezed-state-based schemes, sensitivity enhancement is limited by the loss even for a large amount of squeezing. In this sense, our current scheme with the nonlinear interferometer is less prone to detection loss than squeezed-state-based linear interferometers. The underlining physics for this insensitivity to loss is that the nonlinear interferometer is operated at vacuum-noise level. So the introduction of vacuum noise through losses will change its noise performance. On the other hand, if we inject squeezed vacuum into the unused input port ($\hat{d}_{\rm in}$) to further increase the SNR as in Eq. (14), loss limits the effect of squeezing just like squeezed-state-based schemes.

B. Effect of loss inside the nonlinear interferometer

For losses inside the interferometer, the situation is not so good. We consider two situations: (i) losses in the propagation between the two parametric amplifiers and (ii) losses inside the parametric amplifiers. For the first case, we again model the losses by beam splitters: $\hat{C}' = \sqrt{1 - L_1}\hat{C} + \sqrt{L_1}\hat{C}_0$ and $\hat{D}' = \sqrt{1 - L_2}\hat{D} + \sqrt{L_2}\hat{D}_0$. We also assume the amplifiers have different gains of G_1, G_2, respectively. Then, the idler output port is

$$\hat{d}_{\rm out} = G'(\varphi)\hat{d}_{\rm in} + g'(\varphi)\hat{c}^\dagger_{\rm in} + g_2\sqrt{L_1}\hat{C}^\dagger_0 + G_2\sqrt{L_2}\hat{D}_0, \tag{18}$$

with

$$\begin{aligned}G'(\varphi) &= g_1 g_2\sqrt{1 - L_1} + G_1 G_2 e^{i\varphi}\sqrt{1 - L_2},\\ g'(\varphi) &= g_2 G_1\sqrt{1 - L_1} + g_1 G_2 e^{i\varphi}\sqrt{1 - L_2}.\end{aligned} \tag{19}$$

For strong coherent-state input with $|\alpha|^2 \gg 1$ and

$$g_2 G_1 \sqrt{1-L_1} = g_1 G_2 \sqrt{1-L_2} \equiv gG\sqrt{1-L} \tag{20}$$

for 100% visibility, we find the output intensity as

$$\begin{aligned}\langle \hat{d}^{\dagger}_{\rm out}\hat{d}_{\rm out}\rangle &\approx 2G^2 g^2(1-L)|\alpha|^2(1+\cos\varphi)\\ &= 2G_2^2 I_{ps}^{nl}(1-L_2)(1+\cos\varphi).\end{aligned} \tag{21}$$

So with loss, the fringe size is only reduced by $1-L_2$. However, the quantum noise is not so. With $\varphi = \pi + \delta$ ($\delta \ll 1$), we find from Eq. (18),

$$\begin{aligned}\langle \hat{X}^2_{d_{\rm out}}\rangle &= |g_1 g_2\sqrt{1-L_1} - G_1 G_2 e^{i\delta}\sqrt{1-L_2}|^2\\ &\quad + |g_2 G_1\sqrt{1-L_1} - g_1 G_2 e^{i\delta}\sqrt{1-L_2}|^2 4|\alpha|^2\\ &\quad + G_2^2 L_2 + g_2^2 L_1.\end{aligned} \tag{22}$$

With the condition in Eq. (20) and $\delta \ll 1$, Eq. (22) can be simplified as

$$\langle \hat{X}^2_{d_{\rm out}}\rangle = 1 + 2g_2^2 L_1 + (4|\alpha|^2 + 2)g_1^2 G_2^2(1-L_2)\delta^2. \tag{23}$$

Hence, the SNR is

$$\begin{aligned}R'_{NL} &= (4|\alpha|^2+2)g_1^2 G_2^2(1-L_2)\delta^2\big/\big(1+2g_2^2 L_1\big)\\ &\approx 4I_{ps}^{nl} G_2^2(1-L_2)\delta^2\big/\big(1+2g_2^2 L_1\big).\end{aligned} \tag{24}$$

Compared to Eq. (11) for the case without losses, the SNR is reduced by a factor of $(1-L_2)/(1+2g_2^2 L_1)$ and is compared to the linear interferometer; the enhancement in the SNR is $2G_2^2(1-L_2)/(1+2g_2^2 L_1) \approx 2(1-L_2)/L_1$ for large g_2^2. Thus, like the linear interferometer with a squeezed state, the enhancement is limited by the loss L_1.

Furthermore, for the case of no coherent-state injection, the SNR becomes

$$R_{NL}^{nc'} = 2g_1^2 G_2^2(1-L_2)\delta^2\big/\big(1+2g_2^2 L_1\big), \tag{25}$$

and, for the case of $L_1 = L_2 \equiv L$, is

$$R_{NL}^{nc'} = 2I_{ps}^{nl}\big(I_{ps}^{nl}+1\big)(1-L)\delta^2\big/\big(1+2I_{ps}^{nl}L\big). \tag{26}$$

So, the minimum measurable phase is at the Heisenberg limit for a small photon number with $I_{ps}^{nl} \ll 1/L$, but for the large photon number of $I_{ps}^{nl} \gg 1/L$, Eq. (25) becomes

$$R_{NL}^{nc'} = \big(I_{ps}^{nl}+1\big)(1-L)\delta^2/L, \tag{27}$$

which only improves upon the SQL by $(1-L)/L$, similar to the case of strong coherent injection. This shows that loss is the limiting factor for reaching the Heisenberg limit in precision phase measurement.

The second type of loss of the interferometer is the loss inside the parametric amplifiers. This type of loss cannot be modeled as beam splitters, but parametric amplifiers with internal losses can be characterized as

$$\begin{aligned}\hat{C} &= \bar{G}\hat{c}_{\rm in} + \bar{g}\hat{d}^{\dagger}_{\rm in} + \bar{G}'\hat{c}_0 + \bar{g}'\hat{d}^{\dagger}_0,\\ \hat{D} &= \bar{G}\hat{d}_{\rm in} + \bar{g}\hat{c}^{\dagger}_{\rm in} + \bar{G}'\hat{d}_0 + \bar{g}'\hat{c}^{\dagger}_0,\end{aligned} \tag{28}$$

with $\bar{G}^2 - \bar{g}^2 + \bar{G}'^2 - \bar{g}'^2 = 1$. One example is the nondegenerate optical parametric oscillator below threshold, which acts as a nondegenerate optical parametric amplifier (NOPA) with [23]

$$\begin{aligned}\bar{G} &= [(\gamma^2-\rho^2)/4 + |\kappa|^2]/M, \quad \bar{g} = \kappa\gamma/M,\\ \bar{G}' &= \sqrt{\gamma\rho}(\gamma+\rho)/2M, \quad \bar{g}' = \kappa\sqrt{\gamma\rho}/M,\end{aligned} \tag{29}$$

where κ is proportional to the pump amplitude and γ,ρ is proportional to the cavity round-trip output coupling $\mathcal{T}$ and loss $\mathcal{L}$, respectively, and $M \equiv (\gamma+\rho)^2/4 - |\kappa|^2$. Assuming the second parametric amplifier is identical to the first one, with a phase shift φ on the D field, we have

$$\begin{aligned}\hat{d}_{\rm out} &= \bar{G}_T(\varphi)\hat{d}_{\rm in} + \bar{g}_T(\varphi)\hat{c}^{\dagger}_{\rm in} + \bar{G}'_T(\varphi)\hat{d}_{01}\\ &\quad + \bar{g}'_T(\varphi)\hat{c}^{\dagger}_{01} + \bar{G}'\hat{d}_{02} + \bar{g}'\hat{c}^{\dagger}_{02},\end{aligned} \tag{30}$$

where $\hat{c}_{01},\hat{d}_{01},\hat{c}_{02},\hat{d}_{02}$ are the vacuum modes coupled in through the losses inside the two NOPAs and

$$\begin{aligned}\bar{G}_T(\varphi) &= \bar{g}^2 + \bar{G}^2 e^{i\varphi}, \quad \bar{g}_T(\varphi) = \bar{g}\bar{G}(1+e^{i\varphi}),\\ \bar{G}'_T(\varphi) &= \bar{g}\bar{g}' + \bar{G}\bar{G}' e^{i\varphi}, \quad \bar{g}'_T(\varphi) = \bar{G}'\bar{g} + \bar{G}\bar{g}' e^{i\varphi}.\end{aligned} \tag{31}$$

Then, for $\varphi = \pi + \delta(\delta \ll 1)$ and the strong coherent state at $\hat{c}_{\rm in}$, similar to Eq. (22), we find

$$\begin{aligned}\langle \hat{X}^2_{d_{\rm out}}\rangle &= (\bar{g}^2 - \bar{G}^2)^2 + 4I_{ps}^{nl}\bar{G}^2\delta^2 + (\bar{g}\bar{g}' - \bar{G}\bar{G}')^2\\ &\quad + (\bar{g}\bar{G}' - \bar{G}\bar{g}')^2 + \bar{G}'^2 + \bar{g}'^2\\ &= 4I_{ps}^{nl}\bar{G}^2\delta^2 + 1 + 2(\bar{g}\bar{G}' - \bar{G}\bar{g}')^2 + 2\bar{g}'^2.\end{aligned} \tag{32}$$

where $I_{ps}^{nl} = \langle \hat{D}^{\dagger}\hat{D}\rangle \equiv \bar{g}^2|\alpha|^2$. Hence, the SNR is

$$\begin{aligned}R_{NL}^{nc''} &= 4I_{ps}^{nl}\bar{G}^2\delta^2/(1+4\bar{g}'^2) \approx I_{ps}^{nl}\delta^2\gamma/\rho \quad \text{for } \bar{G} \gg 1\\ &= I_{ps}^{nl}\delta^2\mathcal{T}/\mathcal{L}.\end{aligned} \tag{33}$$

Here, we used Eq. (29). This SNR is enhanced from the SNR (R_L) in Eq. (6) by a factor of $\mathcal{T}/2\mathcal{L}$. Notice that $\mathcal{L}/\mathcal{T} = \mathcal{S}$ is the maximum squeezing from one of the two NOPAs. So the enhancement is limited by the overall vacuum noise leaked into the two parametric amplifiers through intracavity losses.

IV. NONLINEAR MICHELSON INTERFEROMETER WITH PARAMETRIC AMPLIFIERS

Next, let us consider a Michelson interferometer, which is the prototype for gravitational wave detection. We insert parametric amplifiers in its two arms as shown in Fig. 3 and investigate if the nonlinear elements can increase the sensitivity of the interferometer.

In this case, however, we cannot use the parametric amplifiers depicted in Fig. 2(b) because of the extra vacuum noise entering from the unused input port. Instead, we consider a degenerate type of parametric amplifier of the form

$$\hat{C} = G\hat{c}_{\rm in} + g e^{i\varphi_p}\hat{c}^{\dagger}_{\rm in}, \tag{34}$$

where we set $\hat{d} = \hat{c}$ in Eq. (7) to make it degenerate and the amplifier becomes phase sensitive [24] with φ_p as the phase reference ($G,g > 0$). So, referring to Fig. 3, we have the field operators at the free-mass mirrors,

$$\hat{d}_{1,2} = (G\hat{b}_{1,2} + g\hat{b}^{\dagger}_{1,2})e^{i\varphi_{1,2}/2}, \tag{35}$$

where $\varphi_{1,2} = 2k(l_{1,2} + x_{1,2})$ with $l_{1,2}$ as the arm length and $x_{1,2}$ as the displacement of the free masses (m). Then, with

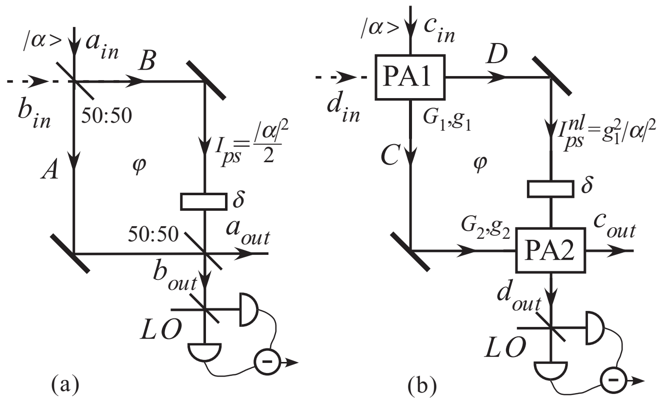

FIG. 2. Comparison between a linear interferometer and a nonlinear interferometer: (a) A linear Mach-Zehnder interferometer. (b) A nonlinear interferometer with parametric amplifiers (PA1, PA2) as the equivalent beam splitters.

the $\hat{d}$ fields propagating back to the parametric amplifier, the outputs of the degenerate parametric amplifiers are

$$\hat{c}_{1,2}^{\rm out} = G_T(\varphi_{1,2})\hat{b}_{1,2} + g_T(\varphi_{1,2})\hat{b}_{1,2}^{\dagger}, \tag{36}$$

with

$$\begin{aligned} G_T(\varphi) &= G^2 e^{i\varphi} + g^2 e^{-i\varphi}, \\ g_T(\varphi) &= Gge^{i\varphi_p}(e^{i\varphi} + e^{-i\varphi}). \end{aligned} \tag{37}$$

As before, the nonlinear parts of the interferometer are operated around unit gain by setting the arm length $l_{1,2}$ such that $2kl_{1,2} = \pi/2 + 2\pi N_{1,2}$ with $N_{1,2}$ as integers. So, $\varphi = \pi/2 + \delta$ ($\delta \equiv 2kx_{1,2} \ll 1$). After dropping the common phase of $\pi/2$, Eq. (37) becomes

$$G_T(\varphi) \approx 1 + i(G^2 + g^2)\delta, \quad g_T(\varphi) \approx 2iGge^{i\varphi_p}\delta, \tag{38}$$

with $\delta = 2kx_{1,2} \ll 1$. For simplicity, we ignore all losses here.

We now send a coherent state $|\alpha\rangle$ into the interferometer in mode $\hat{a}_1^{\rm in}$ and vacuum in the dark port of $\hat{a}_2^{\rm in}$ (Fig. 3). Referring to the inset of Fig. 3, we have

$$\begin{aligned} \hat{b}_1 &= \left(\alpha + \hat{a}_2^{\rm in}\right)/\sqrt{2} \\ \hat{b}_2 &= \left(\hat{a}_2^{\rm in} - \alpha\right)/\sqrt{2}, \end{aligned} \tag{39}$$

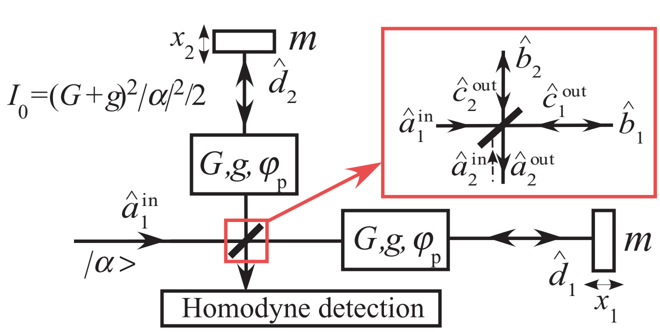

FIG. 3. (Color online) A modified Michelson interferometer with a phase-sensitive amplifier inserted in each arm.

where we treat the strong field of $\hat{a}_1^{\rm in}$ as a classical field. From Eqs. (36) and (38), the outputs from the parametric amplifiers are then

$$\begin{aligned} \hat{c}_1^{\rm out} &\approx \hat{a}_2^{\rm in}/\sqrt{2} + [1 + 2ikx_1(G^2 + g^2 + 2Gge^{i(\varphi_p - 2\varphi_\alpha)})]\alpha/\sqrt{2}, \\ \hat{c}_2^{\rm out} &\approx \hat{a}_2^{\rm in}/\sqrt{2} - [1 + 2ikx_2(G^2 + g^2 + 2Gge^{i(\varphi_p - 2\varphi_\alpha)})]\alpha/\sqrt{2}. \end{aligned} \tag{40}$$

Hence, the dark output port of the modified Michelson interferometer is

$$\begin{aligned} \hat{a}_2^{\rm out} &= \left(\hat{c}_1^{\rm out} + \hat{c}_1^{\rm out}\right)/\sqrt{2} \\ &\approx \hat{a}_2^{\rm in} + i\alpha[G^2 + g^2 + 2Gge^{i(\varphi_p - 2\varphi_\alpha)}]k\Delta x, \end{aligned} \tag{41}$$

with $\Delta x \equiv x_1 - x_2$.

Due to light pressure, the displacement $x_{1,2}$ is related to the photon-number operators of the fields impinging on the free-mass mirrors: $x_{1,2} = \mathcal{C}\hat{d}_{1,2}^{\dagger}\hat{d}_{1,2}$ with $\hat{d}_{1,2}$ as the fields irradiating on the free masses (Fig. 3). $\mathcal{C}$ is the optomechanic constant of free mass m: $\mathcal{C} = \hbar k\tau/m$ [25]. Then, we have

$$\Delta x = x_1 - x_2 = h_{GW} + \mathcal{C}(\hat{d}_1^{\dagger}\hat{d}_1 - \hat{d}_2^{\dagger}\hat{d}_2), \tag{42}$$

where h_{GW} is the signal displacement due to the gravitational wave. From Eq. (35), the photon number in each arm for sensing the motion of the free masses is $I_0 \equiv \langle\hat{d}_{1,2}^{\dagger}\hat{d}_{1,2}\rangle = |\alpha|^2[G^2 + g^2 + 2Gg\cos(\varphi_p - 2\varphi_\alpha)]/2$. Then, from Eqs. (35) and (39), it is straightforward to find

$$\Delta x = h_{GW} + \mathcal{C}|\alpha|\left[(G^2 + g^2)\hat{X}_2^{\rm in}(\varphi_\alpha) + 2Gg\hat{X}_2^{\rm in}(\varphi_p - \varphi_\alpha)\right], \tag{43}$$

where $\hat{X}_2^{\rm in}(\varphi_\alpha) = \hat{a}_2^{\rm in}e^{-i\varphi_\alpha} + \hat{a}_2^{in\dagger}e^{i\varphi_\alpha}$.

The dependence on the phases φ_p,φ_α in Eqs. (41) and (43) and in I_0 for the photon number in each arm is because the degenerate amplifier in Eq. (34) is phase sensitive [24]. So, choosing the phase $\varphi_p - 2\varphi_\alpha = 0$ and substituting Eq. (43) into Eq. (41), we obtain the dark port output,

$$\begin{aligned} X_2^{\rm out} &= X_2^{\rm in} \\ Y_2^{\rm out} &= Y_2^{\rm in} + \mathcal{K}(G+g)^2\hat{X}_2^{\rm in} + \sqrt{2\mathcal{K}(G+g)^2}(h_{GW}/h_{\rm SQL}), \end{aligned} \tag{44}$$

where $X_2^{\rm in} \equiv \hat{X}_2^{\rm in}(\varphi_\alpha)$, $\hat{Y}_2^{\rm in} \equiv \hat{X}_2^{\rm in}(\varphi_\alpha + \pi/2)$, $X_2^{\rm out} \equiv X_2^{\rm out}(\varphi_\alpha) = \hat{a}_2^{\rm out}e^{-i\varphi_\alpha} + \hat{a}_2^{out\dagger}e^{i\varphi_\alpha}$, and $\hat{Y}_2^{\rm out} = \hat{X}_2^{\rm out}(\varphi_\alpha + \pi/2)$. $h_{\rm SQL} \equiv \sqrt{\hbar\tau/m}$ is the SQL, and $\mathcal{K} \equiv 4I_0\hbar k^2\tau/m$ with $I_0 = |\alpha|^2(G+g)^2/2$ as the photon number in each arm.

The quantum-noise performance of a regular Michelson interferometer was analyzed thoroughly in Ref. [9]. Compared to Eq. (16) of Ref. [9], the nonlinear version discussed here has the constant $\mathcal{K}$ increased by $(G+g)^2$-fold under the condition of the same photon number of I_0 in the arms of the interferometer. This will lead to a better performance at the same phase-sensing photon number (I_0). Since we use a single-mode description of the interferometer, we cannot obtain the frequency response for the modified Michelson interferometer discussed here. However, because gravitational-wave bandwidth is much narrower than the bandwidth of nonlinear optical interaction, the gain bandwidth of the parametric amplifiers is much larger than the response bandwidth of the regular Michelson interferometer for gravitational detection, i.e., parameters G,g,φ_p can be treated as constants. So the frequency response of the modified interferometer should be the same as the regular one without the amplifier. A more detailed multimode analysis similar to Ref. [9] confirms this [26]. Therefore, all the benefits for a quantum-non-demolition interferometer discussed in Ref. [9] with a frequency-dependent squeezing angle and a homodyne angle apply here with even better results because of the enhanced $\mathcal{K}$ coefficient.

To be more specific and with full reference to Ref. [9], we may rewrite Eq. (44) as

$$Y_2^{\rm out} = \sqrt{\mathcal{K}'^2+1}\left(Y_2^{\rm in}\sin\theta + \hat{X}_2^{\rm in}\cos\theta\right) + \sqrt{2\mathcal{K}'}(h_{GW}/h_{\rm SQL}), \tag{45}$$

with $\mathcal{K}' \equiv \mathcal{K}(G+g)^2$ and $\cot\theta = \mathcal{K}'$. If we measure $Y_2^{\rm out}$ for the detection of the gravitational signal h_{GW}, the quantum noise is from the first term in Eq. (45), i.e., $\sqrt{\mathcal{K}'^2+1}(Y_2^{\rm in}\sin\theta + \hat{X}_2^{\rm in}\cos\theta)$. The equivalent noise power in measuring h_{GW} then is

$$S_h = \frac{h^2_{\rm SQL}}{2\mathcal{K}'}(1+\mathcal{K}'^2)\langle[\tilde{X}_2^{\rm in}(\theta)]^2\rangle, \tag{46}$$

with $\tilde{X}_2^{\rm in}(\theta) \equiv Y_2^{\rm in}\sin\theta + \hat{X}_2^{\rm in}\cos\theta$. So, if we can squeeze the input field of $\hat{a}_2^{\rm in}$ at the quadrature amplitude $\tilde{X}_2^{\rm in}(\theta)$ with a power-squeeze factor of e^{-2R}, i.e., the squeezing angle is at $\theta_S = {\rm arccot}\,\mathcal{K}'$ [27], Eq. (46) becomes

$$S_h = \frac{h^2_{\rm SQL}}{2}\left(\frac{1}{\mathcal{K}'}+\mathcal{K}'\right)e^{-2R}, \tag{47}$$

which is exactly the same as Eq. (48) in Ref. [9] except replacing $\mathcal{K}$ with $\mathcal{K}' = \mathcal{K}(G+g)^2$. So, with a squeezed-state input at the dark port, the noise power is minimized below the SQL at $\mathcal{K}'=1$ with an optimized circulating photon number of $I_0^{op} = I_{\rm SQL}/(G+g)^2$ ($I_{\rm SQL} \equiv m/4\hbar k^2\tau$). This value is reduced by a factor of $1/(G+g)^2$ as compared to a conventional Michelson interferometer.

For a variational-output interferometer [27], on the other hand, we do not measure $Y_2^{\rm out}$ but rather a different quadrature amplitude $\tilde{Y}_2^{\rm out}(\zeta)$ at a homodyne angle of ζ,

$$\begin{aligned}\tilde{Y}_2^{\rm out}(\zeta) &\equiv Y_2^{\rm out}\sin\zeta + X_2^{\rm out}\cos\zeta \\ &= \sin\zeta\left[Y_2^{\rm in} + X_2^{\rm in}(\cot\zeta+\mathcal{K}') + \sqrt{2\mathcal{K}'}(h_{GW}/h_{\rm SQL})\right].\end{aligned} \tag{48}$$

In this case, we may completely get rid of the $X_2^{\rm in}$ term due to light pressure by choosing a homodyne angle of $\zeta = -{\rm arccot}\,\mathcal{K}'$,

$$S_h^{\rm var} = \frac{h^2_{\rm SQL}}{2\mathcal{K}'}\langle[Y_2^{\rm in}]^2\rangle = \frac{h^2_{\rm SQL}}{2\mathcal{K}(G+g)^2}, \tag{49}$$

if the dark input port is in vacuum. The noise power is reduced further by a factor of $1/(G+g)^2$ beyond the SQL as compared to a conventional variational-output interferometer.

For a squeezed-variational interferometer [27], the input quadrature $Y_2^{\rm in}$ is squeezed, and in the meantime, quadrature $\tilde{Y}_2^{\rm out}(\zeta)$ is measured. From Eq. (49), we have

$$S_h^{\rm sq\text{-}var} = \frac{h^2_{\rm SQL}}{2\mathcal{K}'}\langle[Y_2^{\rm in}]^2\rangle = \frac{h^2_{\rm SQL}}{2\mathcal{K}(G+g)^2}e^{-2R}. \tag{50}$$

To be better than the squeezed-input interferometer given in Eq. (47), we need $\mathcal{K}'>1$ or $I_0 > I_0^{op} = I_{\rm SQL}/(G+g)^2$.

As discussed before, we do not have a frequency-dependent $\mathcal{K}$ here because we use a single-mode treatment. A full multimode treatment [26] can show that the modified Michelson interferometer has the same frequency dependence for $\mathcal{K}$ as the conventional Michelson interferometer as long as the parameters G, g, φ_p are constant within the frequency-response bandwidth of the conventional interferometer. Then, the discussion above will lead to the same frequency-dependent squeezing angle or homodyne angle given in Ref. [9] for squeezed input or variational output or the combination interferometer.

As for the practical implementation of the current scheme for the LIGO project, it is limited by the availability of a parametric amplifier of high-powered cw fields. Current technology in nonlinear optics only can provide stable parametric amplification of a high-powered pulse field. Nevertheless, the current scheme with nonlinear elements inside an interferometer may provide ideas to further improve upon the current LIGO project based on conventional design of interferometers.

V. SUMMARY AND DISCUSSION

To summarize, a nonlinear interferometer with parametric amplifiers as beam splitters has a better SNR in precision phase measurement than a traditional linear interferometer. This improvement is because of the signal enhancement in the nonlinear interferometer. The enhancement factor is not limited by losses outside the interferometer but by the losses inside the interferometer. With squeezed-vacuum input to the unused port, further enhancement can be achieved.

The idea of using nonlinear elements for beam splitting and recombination is not limited to optical interferometry. As a matter of fact, it may not be best suited for an optical interferometer because the sensitivity of an optical interferometer can reach a very high level without resorting to quantum technology due to the availability of a large number of photons, such as the LIGO project. In atomic interferometry, on the other hand, the sensitivity indeed is limited by the number of atoms [28]. Implementation of the ideas in the current paper may well be in an atomic interferometer, which will help to increase the sensitivity tremendously. Recent advances in atom optics made it possible to implement a parametric amplifier for matter waves [29,30].

[1] A. A. Michelson and E. W. Morley, Am. J. Sci. **34**, 333 (1887).

[2] C. M. Caves, Phys. Rev. D **23**, 1693 (1981).

[3] M. Xiao, L. A. Wu, and H. J. Kimble, Phys. Rev. Lett. **59**, 278 (1987).

[4] K. McKenzie, D. A. Shaddock, D. E. McClelland, B. C. Buchler, and P. K. Lam, Phys. Rev. Lett. **88**, 231102 (2002).

[5] H. Vahlbruch, S. Chelkowski, B. Hage, A. Franzen, K. Danzmann, and R. Schnabel, Phys. Rev. Lett. **95**, 211102 (2005).

[6] K. Goda, O. Miyakawa, E. E. Mikhailov, S. Saraf, R. Adhikari, K. McKenzie, R. Ward, S. Vass, A. J. Weinstein, and N. Mavalvala1, Nat. Phys. **4**, 472 (2008).
[7] T. Eberle, S. Steinlechner, J. Bauchrowitz, V. Händchen, H. Vahlbruch, M. Mehmet, H. Müller-Ebhardt, and R. Schnabel, Phys. Rev. Lett. **104**, 251102 (2010).
[8] [http://www.advancedligo.mit.edu].
[9] H. J. Kimble, Y. Levin, A. B. Matsko, K. S. Thorne, and S. P. Vyatchanin, Phys. Rev. D **65**, 022002 (2001).
[10] P. Kok, H. Lee, and J. P. Dowling, Phys. Rev. A **65**, 052104 (2002).
[11] B. Yurke, S. L. McCall, and J. R. Klauder, Phys. Rev. A **33**, 4033 (1986).
[12] J. Jacobson, G. Björk, I. Chuang, and Y. Yamamoto, Phys. Rev. Lett. **74**, 4835 (1995).
[13] Z. Y. Ou, Phys. Rev. A **55**, 2598 (1997).
[14] J. Beltrán and A. Luis, Phys. Rev. A **72**, 045801 (2005).
[15] S. Boixo, S. T. Flammia, C. M. Caves, and J. M. Geremia, Phys. Rev. Lett. **98**, 090401 (2007).
[16] S. M. Roy and S. L. Braunstein, Phys. Rev. Lett. **100**, 220501 (2008).
[17] R. A. Campos, B. E. A. Saleh, and M. C. Teich, Phys. Rev. A **40**, 1371 (1989).
[18] D. Leibfried, B. DeMarco, V. Meyer, M. Rowe, A. Ben-Kish, J. Britton, W. M. Itano, B. Jelenković, C. Langer, T. Rosenband, and D. J. Wineland, Phys. Rev. Lett. **89**, 247901 (2002).
[19] Z. Y. Ou, Phys. Rev. Lett. **77**, 2352 (1996).
[20] W. N. Plick, J. P. Dowling, and G. S. Agarwal, New J. Phys. **12**, 083014 (2010).
[21] J. Jing, C. Liu, Z. Zhou, Z. Y. Ou, and W. Zhang, Appl. Phys. Lett. **99**, 011110 (2011).
[22] M. D. Reid, Phys. Rev. A **40**, 913 (1989).
[23] Z. Y. Ou, S. F. Pereira, and H. J. Kimble, Appl. Phys. B **55**, 265 (1992). We set $\Omega = 0$.
[24] C. M. Caves, Phys. Rev. D **26**, 1817 (1982).
[25] R. Loudon, Phys. Rev. Lett. **47**, 815 (1981).
[26] Z. Y. Ou (unpublished).
[27] See Ref. [9] and references therein for various types of interferometers.
[28] A. D. Cronin, J. Schmiedmayer, and D. E. Prichard, Rev. Mod. Phys. **81**, 1051 (2009).
[29] W. RuGway, S. S. Hodgman, R. G. Dall, M. T. Johnsson, and A. G. Truscott, Phys. Rev. Lett. **107**, 075301 (2011).
[30] C. Gross, T. Zibold, E. Nicklas, J. Estève, and M. K. Oberthaler, Nature (London) **464**, 1165 (2010).